

BRIEF DEFINITIVE REPORT

Nuclear receptor LXR β controls fitness and functionality of activated T cells

Anthony J. Michaels^{1,2*}, Clarissa Campbell^{1*}, Regina Bou-Puerto^{1,2}, and Alexander Y. Rudensky^{1,2}

T cells increase cholesterol biosynthesis upon activation to generate substrates for cellular growth and proliferation. The ubiquitously expressed liver X receptor β (LXR β) encoded by the *Nr1h2* gene is a critical regulator of cholesterol homeostasis in mammalian cells; however, its cell-intrinsic role in T cell biology remains poorly understood. We report that ablation of LXR β in T cells leads to spontaneous T cell activation and T lymphocytopenia. Unexpectedly, analysis of mixed bone marrow chimeric mice revealed a cell-autonomous survival defect that reduced the fitness of LXR β -deficient effector T cells, suggesting that the heightened immune activation in mice harboring LXR β -deficient T cells was due to impaired regulatory T (T reg) cell functionality. Indeed, we found that single-copy deletion of *Nr1h2* in T reg cells disrupted activated T reg cell metabolism and fitness and resulted in early-onset fatal autoimmune disease. Our study demonstrated an indispensable requirement for T reg cell-intrinsic LXR β function in immune homeostasis and provides a basis for immunological therapies through targeting of this receptor.

Introduction

In the context of an immune challenge, newly activated T cells reprogram their metabolism to meet the extraordinary bioenergetic demands of clonal expansion (Geltink et al., 2018). As naive T cells differentiate into effectors, a rewiring of the regulatory networks that govern lipid metabolism ensures the elaboration of cell-mediated immunity (Buck et al., 2015). Lipid oxidation is generally suppressed during the acquisition of effector metabolism in coordination with a reciprocal increase in cholesterol biosynthesis. This anabolic program facilitates the rapid generation of substrates needed for the biosynthesis of molecules supporting cellular proliferation, differentiation, and function. Efficient execution of this process demands a robust system of self-regulation to enable fine tuning of the proliferative response, optimization of metabolite balance, and preservation of overall cellular health (Bietz et al., 2017; Howie et al., 2018). The mechanisms that support metabolic homeostasis during T cell activation and differentiation are not yet fully characterized.

Liver X receptor α (LXR α) and β (LXR β) are negative regulators of cellular cholesterol content and function to limit toxicities associated with cholesterol overabundance. LXR α and LXR β respond to the same ligands and share a high degree of sequence homology in both their DNA- and ligand-binding

domains (Wang and Tontonoz, 2018). While LXR α is the dominant LXR isoform expressed in the liver, adipose tissue, kidney, and macrophages, LXR β is expressed ubiquitously (Bookout et al., 2006). As sterol-responsive nuclear receptors, the LXRs facilitate transcriptional control of gene networks that regulate cholesterol and fatty acid metabolism in response to changes in the abundance of endogenous ligands. Mechanistically, LXR activation by sterol metabolites, including cholesterol derivatives (e.g., oxysterols) and cholesterol precursors (e.g., desmosterol), drives the expression of genes involved in the uptake, transport, efflux, and catabolism of cholesterol and cholesterol metabolites in a tissue-dependent manner (Wang and Tontonoz, 2018).

Several studies have demonstrated a protective role for LXR in animal models of inflammatory disease (Schulman, 2017). For instance, synthetic LXR agonists ameliorate pathology in experimental autoimmune encephalomyelitis, while LXR-deficient animals display exacerbated disease and neuroinflammation (Cui et al., 2011; Hindinger et al., 2006; Xu et al., 2009). Similarly, in a mouse model of allergic contact dermatitis, topical application of an LXR agonist curtails proinflammatory cytokine production and preserves skin morphology (Fowler et al., 2003). Further, LXR-deficient mice are highly susceptible to chemically

¹Howard Hughes Medical Institute and Immunology Program at Sloan Kettering Institute, Ludwig Center for Cancer Immunotherapy, Memorial Sloan Kettering Cancer Center, New York, NY; ²Immunology and Microbial Pathogenesis Graduate Program, Weill-Cornell Graduate School for Medical Sciences, New York, NY.

*A.J. Michaels and C. Campbell contributed equally to this paper; Correspondence to Alexander Y. Rudensky: rudenska@mskcc.org; Clarissa Campbell: campbec2@mskcc.org.

© 2020 Michaels et al. This article is distributed under the terms of an Attribution–Noncommercial–Share Alike–No Mirror Sites license for the first six months after the publication date (see <http://www.rupress.org/terms/>). After six months it is available under a Creative Commons License (Attribution–Noncommercial–Share Alike 4.0 International license, as described at <https://creativecommons.org/licenses/by-nc-sa/4.0/>).

induced colitis, and an LXR agonist treatment suppresses colonic inflammation (Jakobsson et al., 2014). However, despite evidence of strong immunoregulatory activity, knowledge regarding the function of LXR in distinct immune cell types is still lacking. Specifically, the role of LXR β as a cell-intrinsic regulator of T cell differentiation and function remains incompletely defined. In one study, LXR activation with pharmacological ligands was found to inhibit mitogen-driven T cell proliferation, which is in agreement with the reported function of LXR β in suppressing cholesterol biosynthesis (Bensinger et al., 2008). Correspondingly, germline LXR β deficiency results in lymphoid hyperplasia and enhanced lymphocyte responses to antigenic challenge (Bensinger et al., 2008). Although these studies suggest a role for LXR β in restraining T cell activation and function, they fail to address the T cell-intrinsic response to disrupting the physiological regulation of lipid homeostasis by this nuclear receptor.

To address this question, we explored the effect of T cell-restricted LXR β deficiency. We observed that animals with ablation of the *Nr1h2* gene in T cells ($T^{\Delta LXR}$ mice) develop marked T lymphocytopenia and systemic spontaneous T cell activation. Analysis of cell-extrinsic and intrinsic effects of LXR β loss in bone marrow (BM) chimeric mice harboring both LXR β -sufficient and -deficient T cells showed that LXR β -deficient T cells failed to undergo spontaneous activation in the presence of WT Foxp3⁺ regulatory T cells (T reg cells). In these mice, T cells deficient in one or two copies of the receptor coding gene *Nr1h2* displayed a cell-intrinsic fitness defect that was most pronounced in the effector (CD44^{hi}CD62L^{lo}) compartment, suggesting that the increased T cell activation in $T^{\Delta LXR}$ mice was due to impaired T reg cell fitness or function. Indeed, LXR β deficiency restricted to the T reg cell lineage resulted in severe fatal early-onset autoimmune inflammation comparable to that observed in Foxp3-deficient mice. Furthermore, LXR β -deficient T reg cells exhibited dysregulated cholesterol metabolism upon activation. These results highlight a critical requirement for LXR β in the maintenance of metabolic homeostasis and fitness of T cells. Our study suggests that T cells, and T reg cells in particular, may represent major targets for therapeutic LXR modulation and provides a basis for developing novel approaches for the manipulation of immune cell function in disease.

Results and discussion

T cell-specific ablation of LXR β results in T lymphocytopenia and widespread T cell activation

Previous studies of germline LXR β deficiency have suggested a role for this nuclear receptor in the negative regulation of T cell responses (Schulman, 2017). However, in the context of germline deficiency, determining the T cell-intrinsic requirement for LXR β signaling is confounded by cell-extrinsic influences on T cell differentiation and functional states. Therefore, to gain insight into the role of LXR β specifically in T cells, we generated CD4-Cre*Nr1h2*^{fl/fl} ($T^{\Delta LXR}$) mice. In these animals, transgenic Cre recombinase expression is driven by *Cd4* regulatory elements (Lee et al., 2001), resulting in efficient deletion of the loxP-

flanked *Nr1h2* (LXR β) allele in all $\alpha\beta$ T cells in the thymus. $T^{\Delta LXR}$ mice were outwardly healthy and gained weight at a rate comparable to WT *Nr1h2*^{fl/fl} littermate control animals (Fig. 1 A). However, adult $T^{\Delta LXR}$ mice showed a pronounced T lymphocytopenia across all tissues examined (Fig. 1, B and C; and Fig. S1, A and B). In contrast to the decreased TCR β ⁺ T cell numbers, $T^{\Delta LXR}$ mice harbored an enlarged population of $\gamma\delta$ T cells in lymphoid tissues (Fig. S1, C and D). Since the $\gamma\delta$ T lymphocyte lineage is exempt from CD4-Cre-mediated recombination of the *Nr1h2* locus (Shi and Petrie, 2012; Xiong and Raulet, 2007), this observation raises a possibility that LXR β deficiency in $\alpha\beta$ T cells limits their ability to restrict the size of the $\gamma\delta$ T cell compartment either via impaired competition for the T cell niche or by insufficient active restraint in trans. $T^{\Delta LXR}$ mice also harbored an elevated frequency of effector (CD44^{hi}CD62L^{lo}) CD4⁺ and CD8⁺ T cells compared with WT control animals in both lymphoid and nonlymphoid organs (Fig. 1, D and E). Moreover, a greater proportion of effector CD4⁺ and CD8⁺ T cells from $T^{\Delta LXR}$ mice produced the proinflammatory cytokines IFN γ and TNF α upon ex vivo restimulation (Fig. 1 F and Fig. S1, E and F). Notably, the percentage of CD4⁺ T cells producing IL-17 was dramatically increased in all organs examined (Fig. 1 G and Fig. S1 G), while elevated IL-4 production was restricted to barrier sites and their draining LNs (Fig. 1 H and Fig. S1 H).

Given the aberrant expansion of the $\gamma\delta$ T cell population and the systemic increase in effector T cell responses in $T^{\Delta LXR}$ mice, we next profiled their T reg cell compartment. $T^{\Delta LXR}$ mice showed reduced numbers of Foxp3⁺ CD4⁺ T cells relative to WT control animals (Fig. 1 I). This reduction tracked with the total peripheral TCR β ⁺ T cell population, whose size was also diminished approximately sixfold in $T^{\Delta LXR}$ mice relative to WT controls (Fig. 1, B and I). Accordingly, the frequency of Foxp3⁺ T reg cells among CD4⁺ T cells was unchanged (Fig. 1 J). CD4-Cre transgene activity is initiated at the CD4CD8 double-positive (DP) thymocyte stage of T cell differentiation (Shi and Petrie, 2012), preceding the induction of Foxp3 expression in T reg cell precursors. Analyses of thymocytes revealed reduced numbers of CD4 single-positive (SP) and Foxp3⁺ cells in $T^{\Delta LXR}$ mice compared with WT littermates (Fig. S1, I and J) and no detectable alterations of double-negative (DN), DP, and CD8SP cell compartments (Fig. S1 I). Compared with WT, $T^{\Delta LXR}$ thymi displayed a selective accumulation of the CD25⁺Foxp3⁻ CD4SP population, which is highly enriched for T reg cell precursors, and a concomitant reduction in CD25⁺Foxp3⁺ CD4SP cells comprising the next and final stage of thymic T reg cell maturation (Fig. S1 K). These results suggest that developmental defects in $T^{\Delta LXR}$ mice may contribute to the decreased numbers of CD4⁺ and T reg cells in the periphery. Overall, these findings indicate that LXR β ablation in the $\alpha\beta$ T cell lineage results in T lymphocytopenia and spontaneous T cell activation and that LXR β is required for the homeostasis of both conventional and Foxp3⁺ T cells.

LXR β -deficient T cells are unfit and display a survival defect in the effector compartment in competitive settings

Analysis of $T^{\Delta LXR}$ mice revealed a profound effect of LXR β deficiency on the numbers and activation status of CD4⁺ and CD8⁺ T cells. We considered the possibility that the lymphopenic

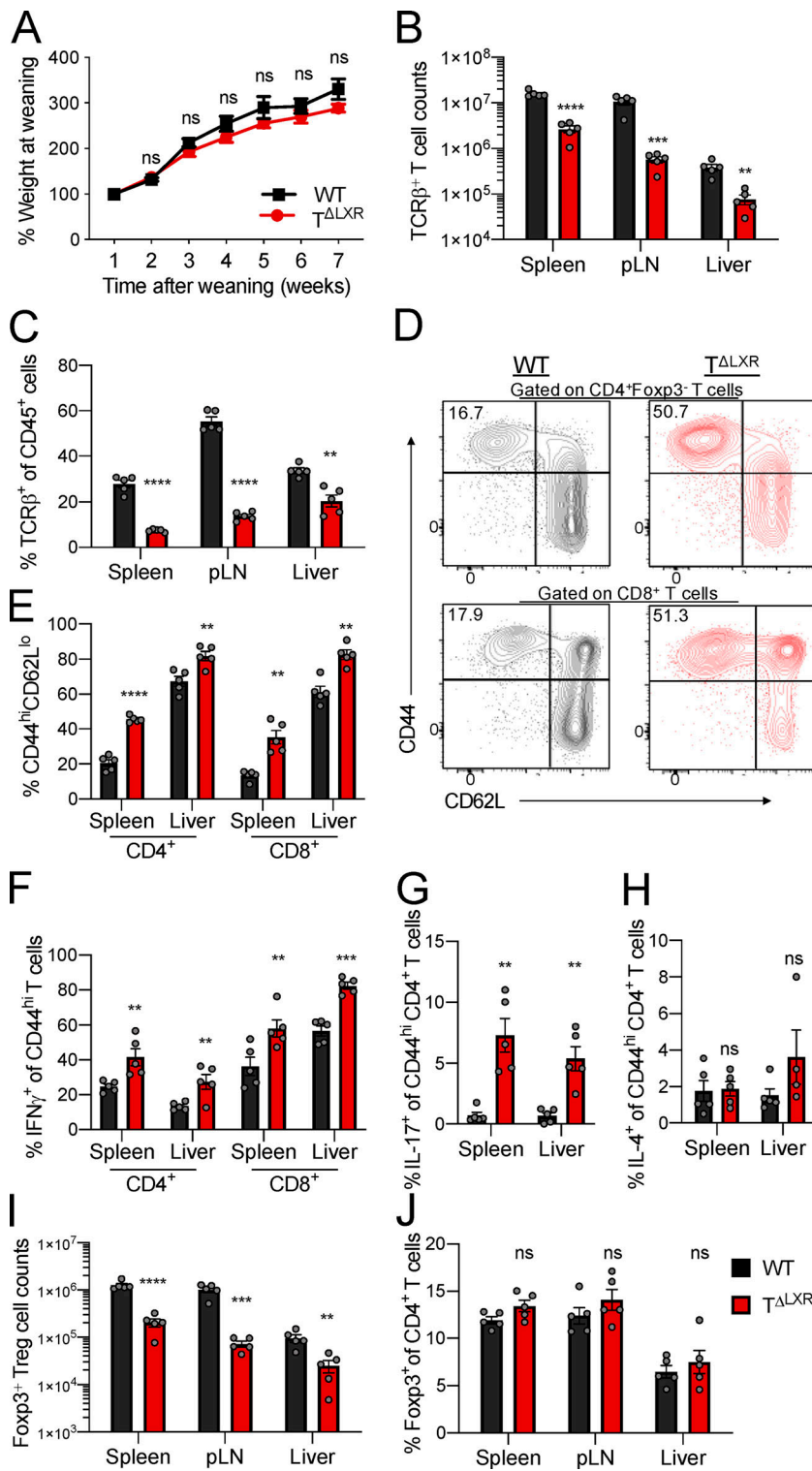


Figure 1. T cell-specific ablation of LXRβ results in T lymphocytopenia and spontaneous T cell activation. (A–J) Analysis of 6–8-wk-old CD4-Cre*Nr1h2*^{fl/fl} (T^{ΔLXR}) and *Nr1h2*^{fl/fl} (WT) littermate mice. (A) Weight gain plotted as percentage of weight at weaning (4 wk old). (B) Quantification of TCRβ⁺ T cell numbers in spleen, pLN, and liver. (C) Frequency of TCRβ⁺ T cells among CD45⁺ cells. (D and E) Representative flow cytometry plots (D) and percentages (E) of effector (CD44^{hi}CD62L^{lo}) CD4⁺ and CD8⁺ T cells. (F–H) Frequency of effector T cells producing the indicated cytokines upon ex vivo restimulation with PMA and ionomycin in the presence of brefeldin A and monensin. (F) Percentages of CD4⁺ and CD8⁺ effector T cells producing IFNγ. (G and H) Percentages of effector CD4⁺ T cells producing IL-17 (G) or IL-4 (H). (I and J) Cell numbers (I) and frequencies (J) of Fopx3⁺ T reg cells in indicated organs. Data presented as mean ± SEM (n = 5). ns, nonsignificant = P > 0.05; **, P < 0.01; ***, P < 0.001; ****, P < 0.0001. Statistical significance was determined using one-way ANOVA followed by the Holm-Šidák correction. Data are representative of at least three independent experiments.

environment in T^{ΔLXR} mice could contribute to the increased activation of LXRβ-deficient T cells. To address this hypothesis, we cotransferred bulk WT and LXRβ-deficient T cells into T cell-deficient (*Tcrb*^{-/-}/*Tcrd*^{-/-}) recipients and analyzed them 7 d later. We did not observe a relative increase in the frequency of CD44^{hi}CD62L^{lo} cells derived from the LXRβ-deficient donor (Fig. S2 A), suggesting that loss of LXRβ does not exacerbate T cell activation in lymphopenic settings.

Since the size of the Fopx3⁺ T reg cell population was also severely diminished upon LXRβ ablation, the spontaneous T cell activation phenotype in T^{ΔLXR} mice could be a consequence of defective T reg cell function rather than a reflection of a previously proposed cell-autonomous role of LXRβ in limiting activation of conventional T cells (Bensinger et al., 2008). To distinguish between these two nonmutually exclusive possibilities, we generated mixed BM chimeric mice by transferring BM

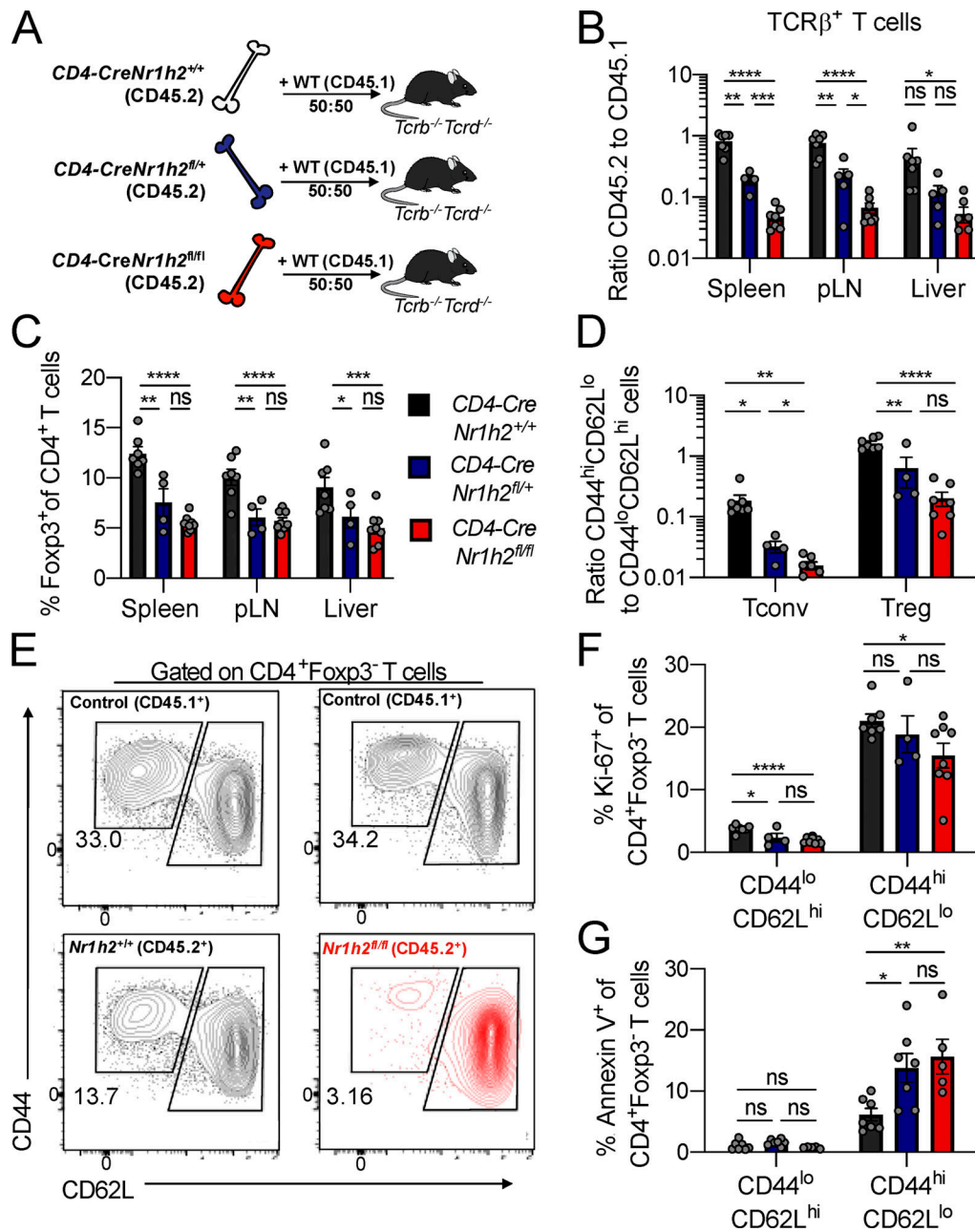


Figure 2. LXRβ-deficient T cells are competitively unfit. (A–G) CD45.2⁺ BM precursor cells from CD4-CreNr1h2^{+/+}, CD4-CreNr1h2^{fl/+}, or CD4-CreNr1h2^{fl/fl} animals were mixed at a 1:1 ratio with CD45.1⁺ calibrator cells from WT donors and transferred into lethally irradiated mice. Recipients were analyzed 8 wk after reconstitution. (A) Experimental design of mixed BM chimera experiments. (B) Ratio of CD45.2⁺ to CD45.1⁺ T cell numbers in indicated tissues. (C) Percentages of Foxp3⁺ T reg cells as a fraction of CD4⁺ T cells within the CD45.2⁺ compartment at the indicated organs. (D) Ratio of effector (CD44^{hi}CD62L^{lo}) to resting (CD44^{lo}CD62L^{hi}) T reg (CD4⁺Foxp3⁺) and conventional (CD4⁺Foxp3⁻) T cell numbers in the spleen. (E) Representative flow cytometry plots showing the activation status of recipient-matched CD45.2⁺ (CD4-CreNr1h2^{+/+} or CD4-CreNr1h2^{fl/fl}) and CD45.1⁺ (WT control) T cells. (F and G) Quantification of Ki-67⁺ (F) and Annexin V⁺ (G) conventional CD4⁺T cells in the spleen. Data are presented as mean ± SEM (n = 4–7). ns, nonsignificant = P > 0.05; *, P < 0.05; **, P < 0.01; ***, P < 0.001; ****, P < 0.0001. Statistical significance was determined using one-way ANOVA followed by the Holm-Šidák correction. Data are representative of at least three independent experiments.

progenitor cells derived from CD4-CreNr1h2^{+/+}, CD4-CreNr1h2^{fl/+}, or CD4-CreNr1h2^{fl/fl} animals (CD45.2⁺) at a 1:1 ratio with BM progenitor cells from congenically marked WT donors (CD45.1⁺) into lethally irradiated *Tcrb*^{-/-}*Tcrd*^{-/-} animals (Fig. 2 A). As a result, the CD45.2⁺ compartment in chimeric mice contained T cells that were LXRβ sufficient (CD4-CreNr1h2^{+/+}), heterozygous (CD4-CreNr1h2^{fl/+}), or deficient (CD4-CreNr1h2^{fl/fl}), whereas

the CD45.1 compartment consistently contained WT T cells. This strategy allowed us to test the cell-intrinsic effects of LXRβ ablation and *Nr1h2* gene dosage in an environment that also harbors a population of LXRβ-sufficient T reg cells to restrain systemic inflammation.

In agreement with results from T^{ΔLXR} animals, analysis of mixed BM chimeric mice revealed a debilitating effect of LXRβ

deficiency on T cell numbers. While in control BM chimeras we observed comparable numbers of CD4-Cre*Nr1h2*^{+/+} T cells and CD45.1⁺ WT control cells, CD4-Cre*Nr1h2*^{fl/+} and CD4-Cre*Nr1h2*^{fl/fl} T cells showed a marked competitive disadvantage in a gene dose-dependent manner (Fig. 2 B). LXRβ deficiency also resulted in a profound reduction in T reg cell frequencies (Fig. 2 C). Despite that, WT CD45.1⁺ T cells displayed a consistent ratio of activated to naive T cells across all recipient groups (Fig. S2 B), indicating that inflammatory responses were well controlled in mixed BM chimeric mice. Flow cytometric analysis revealed that in contrast to the heightened T cell activation observed in T^{ΔLXR} mice, LXRβ-deficient CD4⁺ effector T cells were severely underrepresented in comparison to their naive counterparts in the secondary lymphoid organs of the corresponding BM chimeras (Fig. 2, D and E; and Fig. S2 C). Similarly, the size of the CD44^{hi}CD62L^{lo} population was also decreased among LXRβ-deficient T reg cells (Fig. 2 D). Of note, within the LXRβ-deficient T cell population, we observed sharply increased effector CD4⁺ and CD8⁺ T cell to T reg cell ratios in both lymphoid and nonlymphoid tissues (Fig. S2, D and E), suggesting that T reg cells may exhibit higher dependence on LXRβ relative to their effector counterparts. These results suggest that the T lymphocytopenia observed in T^{ΔLXR} mice was caused by a cell-intrinsic requirement for LXRβ to support cellular homeostasis, while the increased T cell activation likely results from diminished T reg cell numbers and functional activity.

We next investigated how T cell-intrinsic LXRβ ablation caused a reduction in effector T cell numbers. In contrast to a previous study reporting a proliferative advantage of T cells obtained from total body LXRβ-deficient animals (Bensinger et al., 2008), we found that LXRβ deficiency decreased homeostatic proliferation in both the resting and activated T cell compartments as measured by Ki-67 staining (Fig. 2 F). To assess whether LXRβ deficiency compromised cell survival, we performed ex vivo Annexin V staining on cells isolated from mixed BM chimeras. We found that a greater proportion of LXRβ-deficient activated and effector CD4⁺ T cells stained positive for Annexin V compared with WT cells (Fig. 2 G and Fig. S2 F). In contrast, we did not observe increased Annexin V staining within the naive cell compartment (Fig. 2 G and Fig. S2 F), indicating that the LXRβ-dependent survival defect is specific to cells that have experienced activation. Altogether, these findings suggest that LXRβ expression supports the homeostasis of both conventional and Foxp3⁺ T cells and indicate a strong requirement for this nuclear receptor in the effector T cell compartment.

Cell-intrinsic expression of LXRβ regulates T cell survival upon activation

The impact of LXRβ deficiency on effector T cells prompted us to investigate the role of this nuclear receptor during T cell activation. Upon receiving signals through their TCR, naive T cells become activated and exit quiescence, undergoing clonal expansion. To directly assess whether LXRβ deficiency affects activation-induced proliferation, we FACS purified naive CD4-Cre*Nr1h2*^{+/+}, CD4-Cre*Nr1h2*^{fl/+}, and CD4-Cre*Nr1h2*^{fl/fl} CD4⁺ T cells and assessed CellTrace Violet dilution upon in vitro stimulation

with CD3 and CD28 antibody-coated beads in the presence of IL-2. We found that LXRβ-deficient T cells failed to proliferate to the same extent as WT (Fig. 3 A). The viability of activated T cells lacking LXRβ was significantly diminished relative to LXRβ-sufficient cells (Fig. 3 B), corroborating our in vivo observations (Fig. 2 G).

During the differentiation of effector T cells, the regulatory networks that control lipid metabolism favor increased cholesterol biosynthesis (Pearce, 2010). In the absence of LXRβ, a negative regulator of cellular cholesterol content, we expected that T cells would accumulate cholesterol upon activation. To test this assumption, we assessed free cholesterol levels in in vitro activated T cells by flow cytometry using the naturally fluorescent polyene antibiotic filipin III. Filipin binding requires the presence of a free 3'OH group on its sterol interactants. Therefore, the reagent does not recognize esterified cholesterol (Gimpl, 2010; Muller et al., 1984). LXRβ-deficient cells showed increased filipin staining compared with WT control cells 24 h after activation (Fig. 3 C). Given the impact of cholesterol content on plasma membrane fluidity and TCR signaling (Klammt and Lillemeier, 2012), we sought to assess whether early T cell activation events were comparable between LXRβ-sufficient and -deficient cells. The frequency of cells expressing the early T cell activation marker CD69 was similar across all three genotypes at 3 and 6 h after activation (Fig. 3 D). Furthermore, expression of the transcription factor Egr2, which is induced by TCR stimulation in a manner proportional to TCR signal strength, was not affected by LXRβ deficiency 24 h after activation (Fig. 3 E). Correspondingly, phosphorylation of the S6 ribosomal protein, a target of mTOR activation downstream of the TCR and cytokine receptor signaling, was equivalent between LXRβ-sufficient and deficient cells (Fig. 3 F). These results suggest that differences in cell viability and proliferation are likely not a consequence of altered TCR signaling.

Since LXRβ-deficient T cells showed increased cholesterol content following activation, we sought to determine whether disrupted cholesterol homeostasis contributed to their reduced proliferative capacity. At the level of synthesis, cholesterol abundance is determined by the rate-controlling enzyme 3-hydroxy-3-methyl-glutaryl-coenzyme A reductase (HMGCR). To test whether deregulated cholesterol production in the context of LXRβ ablation affected T cell proliferation, we inhibited endogenous cholesterol synthesis using the HMGCR inhibitor simvastatin (Simva) and provided LXRβ-sufficient and -deficient cells with the same amount of the immediate downstream product of HMGCR, mevalonate. Mevalonate partially restored the proliferation of WT and LXRβ-deficient cells treated with Simva at 48 h after activation (Fig. 3 G), indicating that exogenous provision of a cholesterol precursor can overcome HMGCR inhibition independently of LXRβ expression. However, this strategy failed to mitigate differences between genotypes compared with no treatment, suggesting that the proliferative defect in LXRβ-deficient cells may involve processes downstream of mevalonate synthesis or additional, cholesterol-independent mechanisms.

Next, we investigated the mechanisms mediating enhanced cell death upon activation in the absence of LXRβ. Loss of

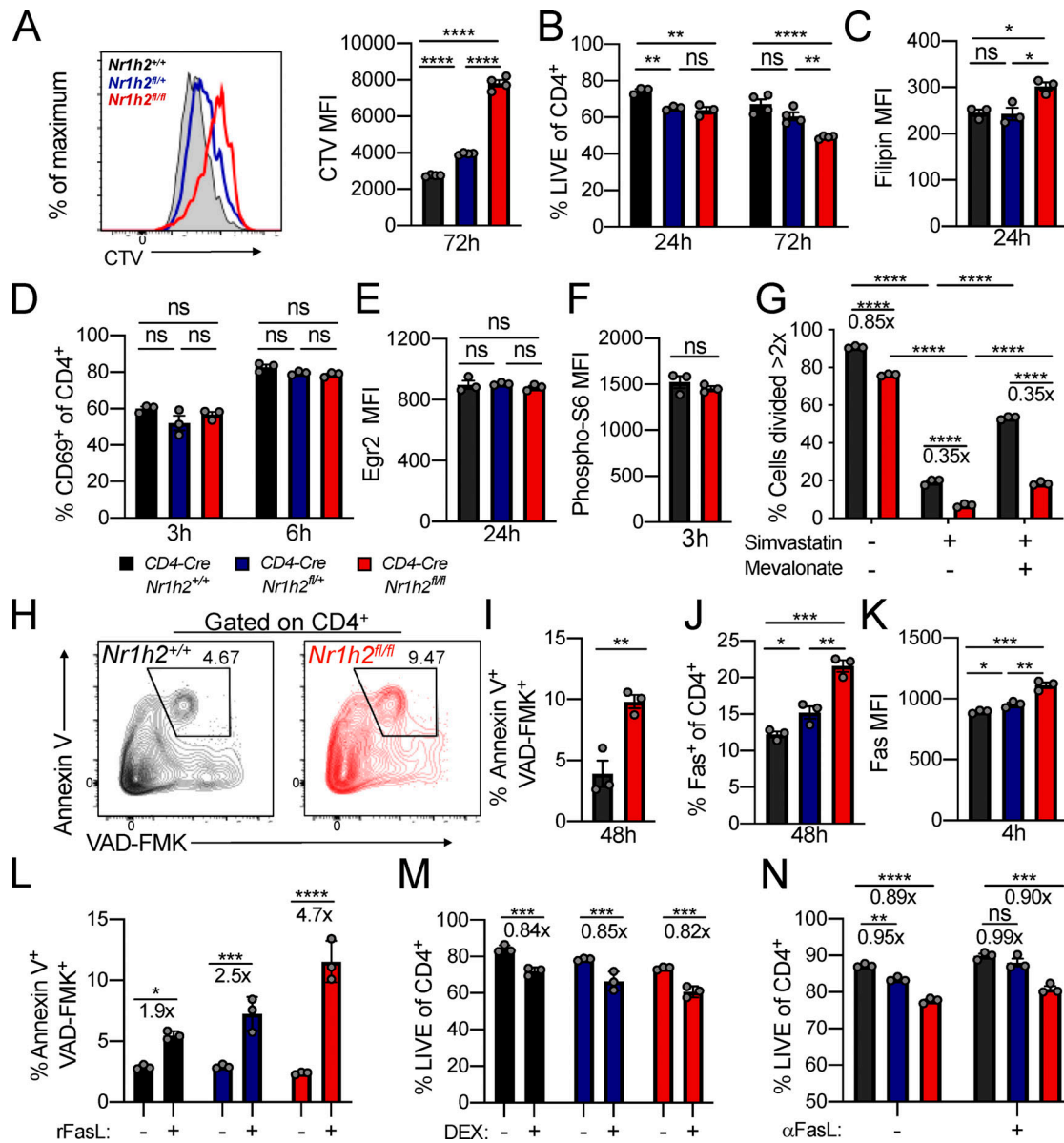


Figure 3. Cell-intrinsic expression of LXR β regulates T cell survival upon activation. (A–N) Naive CD4⁺ T cells sorted from CD4-Cre*Nr1h2*^{+/+}, CD4-Cre*Nr1h2*^{fl/fl}, or CD4-Cre*Nr1h2*^{fl/fl} mice were activated in vitro with CD3 and CD28 antibody-coated beads in the presence of 100 U/ml IL-2 and analyzed at the indicated time points. **(A)** Representative histogram (left) and quantification of mean fluorescence intensity (MFI; right) of CellTrace Violet (CTV) label dilution 72 h after activation. **(B)** Percentages of live cells in culture. **(C)** Filipin III MFI. **(D)** Percentage of cells expressing CD69. **(E and F)** Expression of Egr2 (E) and phosphorylated S6 (F) by indicated cell types. The data are shown as MFI. **(G)** Percentages of cells that divided more than twice in the presence of Simva (10 μ M) and mevalonate (1 mM) 48 h after activation. **(H and I)** Representative flow cytometry plots (H) and percentage (I) of Annexin V⁺ Z-VAD-FMK⁺ cells 48 h after activation. **(J)** Percentages of cells expressing Fas. **(K)** Fas MFI. **(L)** Percentages of Annexin V⁺ Z-VAD-FMK⁺ cells after 4 h incubation with recombinant FasL. **(M and N)** Percentages of live cells after 48-h treatment with 1 μ M dexamethasone (DEX; M) or FasL blocking antibody (N). Data are presented as mean \pm SEM ($n = 3$). Ns, nonsignificant = $P > 0.05$; *, $P < 0.05$; **, $P < 0.01$; ***, $P < 0.001$; ****, $P < 0.0001$. Statistical significance was determined using one-way ANOVA (A–E, J–K, and N), two-way ANOVA (G), or multiple t tests (F and I) followed by the Holm-Šidák correction. Data are representative of at least two independent experiments.

viability in LXR β -deficient cells was accompanied by greater Annexin V and cleaved caspase staining, which are suggestive of increased apoptosis upon activation (Fig. 3, H and I). Since Fas localizes to cholesterol-rich membrane domains and plays a role in the apoptosis of activated lymphocytes (Legembre et al., 2006), we assessed the contribution of this pathway to the death of activated T cells in the context of LXR β deficiency. Compared with WT, LXR β -deficient cells showed increased Fas

staining 4 h after activation (Fig. 3, J and K). Consistently, cross-linking of Fas with recombinant influenza hemagglutinin (HA)-tagged FasL and HA antibody-coated beads induced apoptosis in a higher fraction of LXR β -deficient cells compared with WT (Fig. 3 L). Cell death induced by dexamethasone was comparable between the two genotypes at 48 h (Fig. 3 M), suggesting specific susceptibility to Fas-induced apoptosis. Despite these results, abolishing Fas/FasL interaction using a FasL blocking

antibody led to similar increases in T cell viability in the presence or absence of LXR β (Fig. 3 N). These findings suggest that the Fas/FasL pathway may not solely account for the survival defect of LXR β -deficient cells even though these cells exhibit increased susceptibility to Fas-mediated cell death. Altogether, these experiments suggest that LXR β regulates cholesterol homeostasis in activated T cells and is required for the survival and expansion of effector cells.

LXR β deficiency affects T reg cell differentiation and fitness

Our mixed BM chimera experiments demonstrated a cell-intrinsic role for LXR β in maintaining T cell fitness, with an especially pronounced effect on the effector T cell compartment. However, since naive T cells were also affected (Fig. S2 C), we sought to determine whether differences in cell fitness were already apparent during thymic development. Starting from the DP stage, CD4-Cre*Nr1h2*^{fl/fl} cells showed a competitive disadvantage that persisted through the CD4SP and CD8SP thymocyte stages (Fig. S3, A and B). Contrary to the notable effect of LXR β haploinsufficiency on the competitive fitness of peripheral T cells (Fig. 2 B), loss of a single copy of the *Nr1h2* gene had no effect on DP, CD4SP, and CD8SP thymocytes, as their relative abundance was similar to that of WT cells (Fig. S3 B). Accordingly, CD4-Cre*Nr1h2*^{fl/fl} thymocytes, but not CD4-Cre*Nr1h2*^{fl/+} CD4SP and CD8SP thymocytes, displayed elevated Annexin V staining (Fig. S3 C), indicative of increased apoptosis. Notably, LXR β deficiency resulted in a gene dose-dependent reduction in the frequency of Foxp3⁺ cells among CD4SP thymocytes (Fig. S3 D), consistent with the heightened dependency on LXR β observed for peripheral T reg cells (Fig. S2, D and E). The accumulation of Foxp3⁺ cell precursors and depletion of mature T reg cells observed in the thymi of T^{ΔLXR} animals (Fig. S1 K) was similarly present in LXR β -deficient thymocytes in mixed BM chimeric mice and also showed gene dose dependency (Fig. S3, E and F). Altogether, these data suggest that deletion of a single copy of the *Nr1h2* gene has a pronounced debilitating effect on the fitness of T reg cells and conventional CD4⁺ T cells in the periphery while selectively impairing thymic T reg cell generation.

T reg cell-specific deletion of LXR β results in early-onset fatal autoimmune inflammation

The results above raised the question of whether impaired induction of the *Foxp3* gene in LXR β -deficient thymic T reg cell precursors limits the peripheral T reg cell pool and drives effector T cell activation and cytokine production in T^{ΔLXR} mice. Alternatively, spontaneous T cell activation in these animals could be due to increased T reg cell dependency on LXR β compared with effector T cells. To directly test if perturbation of LXR β signaling in T reg cells after Foxp3 induction affects their fitness and functionality, we restricted LXR β deficiency to the T reg cell lineage by generating Foxp3^{YFP-Cre}*Nr1h2*^{fl} mice. Strikingly, we found that loss of even a single copy of the *Nr1h2* gene in T reg cells caused early-onset fatal autoimmune inflammatory disease similar to that observed in Foxp3-deficient animals (Fig. 4 A). Foxp3^{Cre/y}*Nr1h2*^{fl/+} males presented with severe inflammation and mononuclear cell infiltration affecting skin, lung, and liver

(Fig. 4 B). In comparison to Foxp3^{Cre/y}*Nr1h2*^{+/+} WT littermate controls, the diseased Foxp3^{Cre/y}*Nr1h2*^{fl/+} mice displayed a massive increase in effector T cell responses, including sharply augmented production of all three major types of proinflammatory cytokines upon ex vivo restimulation (Fig. 4, C and D). Although these animals harbored a population of T reg cells, *Nr1h2* haploinsufficiency compromised their ability to scale with the effector T cell populations to restrain proinflammatory responses (Fig. 4 E). Thus, T reg cell numbers and their ability to limit effector T cell responses and the ensuing inflammation are critically impaired by ablation of a single copy of the *Nr1h2* gene.

LXR β -deficient T reg cells are functionally impaired

The severe disease observed in mice harboring LXR β -deficient T reg cells confounds direct comparison of cellular phenotypes between affected experimental animals and healthy controls due to cell-extrinsic effects of systemic inflammation (van der Veeken et al., 2016). Therefore, we generated mosaic female Foxp3^{YFP-Cre/Thy1.1}*Nr1h2*^{fl/+} mice that harbor T reg cells expressing one or two functional copies of *Nr1h2* gene. In these animals, LXR β -sufficient Thy1.1⁺ T reg cells restrain systemic inflammation because they lack Cre expression due to random inactivation of the X-linked *Foxp3* gene (Josefowicz et al., 2012).

In agreement with mixed BM chimera experiments, we observed a competitive disadvantage associated with LXR β deficiency in YFP⁺ (*Nr1h2*^{-/-}) T reg cells in female Foxp3^{YFP-Cre/Thy1.1}*Nr1h2*^{fl/+} mice (Fig. 5, A and B). Notably, control female Foxp3^{YFP-Cre/Thy1.1}*Nr1h2*^{+/+} mice harbored similar numbers of YFP⁺ and Thy1.1⁺ T reg cells, suggesting that this fitness defect was not caused by differences in Foxp3 expression driven by the two *Foxp3* reporter alleles (Fig. 5 A; Bettini et al., 2012; Darce et al., 2012). We also observed a relative depletion of activated CD44^{hi}CD62L^{lo} cells among LXR β -deficient T reg cells in the secondary lymphoid organs of Foxp3^{YFP-Cre/Thy1.1}*Nr1h2*^{fl/+} mice (Fig. 5 C). This reduction was coupled with a decreased percentage of cells expressing molecules associated with T reg cell suppressive capacity and fitness. For example, the percentage of activated *Nr1h2*^{-/-} T reg cells expressing high amounts of CD25 was diminished (Fig. 5 D), while levels of this protein were comparable on resting CD44^{lo}CD62L^{hi} *Nr1h2*^{-/-} and *Nr1h2*^{+/+} T reg cells. Additionally, decreased expression of the activation-induced inhibitory receptor programmed cell death 1 (PD-1) in both the resting and activated T reg cell compartments suggested that LXR β -deficiency likely affects the early stages of T reg cell activation (Fig. 5 E). These results indicate that the functionality of *Nr1h2*^{-/-} T reg cells may be compromised by failure to acquire an effector phenotype and by decreased expression of suppressive molecules.

Thymic T reg cells recognize self-antigens with moderate to high affinity and require continuous TCR signaling for their homeostasis (Josefowicz et al., 2012; Levine et al., 2014). Consistent with the increase in free cholesterol levels observed upon activation of LXR β -deficient conventional T cells, filipin III staining revealed markedly higher cholesterol content in activated, but not resting, LXR β -deficient *Nr1h2*^{-/-} T reg cells relative to their LXR β -sufficient counterparts (Fig. 5 F). Since both conventional CD4⁺ and T reg cells displayed defective cholesterol

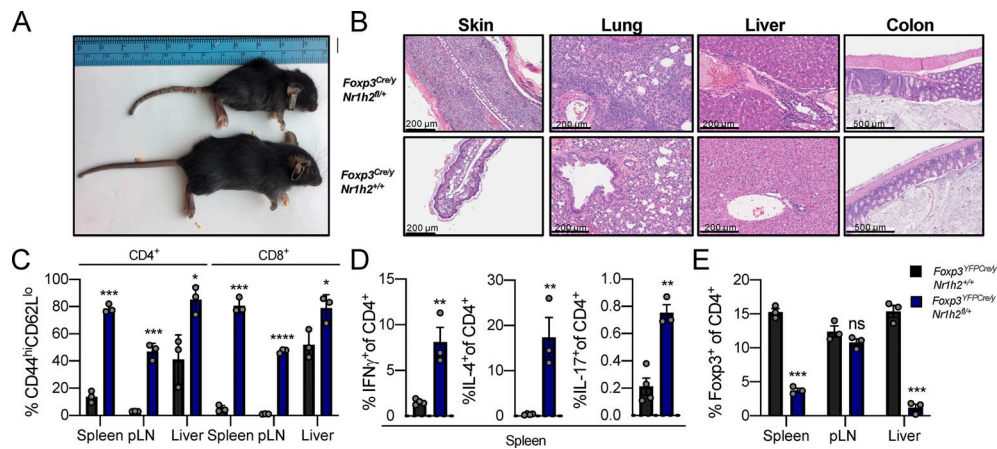


Figure 4. T reg cell-specific deletion of LXR β results in early-onset fatal autoimmune inflammation. (A–E) Characterization of autoimmune disease in 4-wk-old *Foxp3^{Cre/ey}Nr1h2^{fl/+}* mice. **(A)** Appearance of 4-wk-old *Foxp3^{Cre/ey}Nr1h2^{fl/+}* (top) and *Foxp3^{Cre/ey}Nr1h2^{+/-}* (bottom) littermates. **(B)** Hematoxylin and eosin staining of skin, lung, liver, and colon from 4-wk-old *Foxp3^{Cre/ey}Nr1h2^{fl/+}* (top row) and *Foxp3^{Cre/ey}Nr1h2^{+/-}* (bottom row) mice. **(C)** Percentages of CD44^{hi}CD62L^{lo} effector T cells as a fraction of cells within indicated compartment. **(D)** Percentages of splenic CD4⁺ T cells producing proinflammatory cytokines (IFN γ , IL-4, and IL-17) upon ex vivo restimulation with PMA and ionomycin in the presence of brefeldin A and monensin. **(E)** Percentages of Fopx3⁺ T reg cells among CD4⁺ T cells. Data are presented as mean \pm SEM ($n = 3$). ns, nonsignificant = $P > 0.05$; *, $P < 0.05$; **, $P < 0.01$; ***, $P < 0.001$; ****, $P < 0.0001$. Statistical significance was determined using a two-tailed t test (D) or multiple T tests followed by the Holm-Sídák correction (C and E). Data are representative of at least three independent experiments.

homeostasis upon activation, we sought to investigate potential causes for their differential sensitivity to LXR β gene dosage. Analysis of *Nr1h2* mRNA levels in resting T reg cells and conventional CD4⁺T cells by real-time quantitative PCR revealed similar gene expression (Fig. 5 G). Compared with conventional CD4⁺T cells, T reg cells showed increased levels of *Nr1h2* mRNA upon activation (Fig. 5 G). The expression of the cholesterol efflux transporters *Abca1* and *Abg1* is directly controlled by LXR β (Wang and Tontonoz, 2018). We found that while both T reg cells and conventional CD4⁺ T cells down-regulated *Abca1* and *Abg1* transcript levels following activation, T reg cells maintained higher expression of these genes compared with conventional CD4⁺ T cells (Fig. 5, H and I), suggesting cell-type-specific differences in the regulation of cholesterol metabolism. Overall, our findings indicate that T reg cells are severely impaired by LXR β deficiency and that the resulting cholesterol accumulation may affect their survival and fitness upon activation.

Concluding remarks

Our study revealed a cell-intrinsic requirement for LXR β in T cell homeostasis. We found that T cell-restricted deletion of LXR β results in spontaneous T cell activation and profound T lymphocytopenia affecting the conventional and Fopx3⁺ T cell lineages. LXR β deficiency disproportionately affected the survival of effector, but not naive, T cells. Consistently, LXR β -deficient T cells exhibited increased cholesterol content coupled with decreased viability and proliferation following activation. It is likely that reduced cell fitness following antigenic stimulation contributes to the severe T lymphocytopenia in T Δ LXR mice, which is aggravated by reduced T reg cell functionality and consequentially increased levels of spontaneous T cell activation. Our findings are at odds with previous reports that implicated LXR β as a negative regulator of T cell proliferation (Bensinger

et al., 2008). Although activation of LXR with synthetic agonists was reported to inhibit T cell expansion, pharmacological agents disrupt the feedback regulation of LXR β by endogenous ligands and may therefore confound the understanding of its physiological role in proliferating lymphocytes. Mice harboring LXR β -deficient T reg cells succumbed to fatal autoinflammatory disease, highlighting a critical role for LXR β in T reg cell fitness and functional competence. The latter is conditional upon continuous TCR signaling in response to self-antigens to promote the generation of suppressive “effector” T reg cells with an activated phenotype, which were more disproportionately affected by LXR β deficiency (Levine et al., 2014; Vahl et al., 2014). Notably, the T reg cell compartment was more severely disabled by a loss of a single copy of *Nr1h2* gene compared with conventional T cells. This differential metabolic vulnerability of T reg and effector T cells makes LXR β a potential target for therapeutic manipulation. Altogether, our study uncovered a critical immunoregulatory role for LXR β in T cell biology.

Materials and methods

Mice

Experiments in this study were approved by the Sloan Kettering Institute Institutional Animal Care and Use Committee under protocol 08–10–023. Mice were housed at the Sloan Kettering Institute animal facility under specific pathogen-free conditions on a 12-h light/dark cycle with free access to water and regular chow diet (PicoLab; 5053). All control and experimental animals were age matched, and littermates were used as controls unless otherwise indicated. CD4-Cre (Lee et al., 2001), *Foxp3^{YFP-Cre}* (Rubtsov et al., 2008), *Foxp3^{Ttyl1}* (Liston et al., 2008), and *Tcrb^{-/-}Tcrd^{-/-}* mice were purchased from The Jackson Laboratory and maintained in house. C57BL/6-Ly5.1 (CD45.1) mice were obtained from Charles River Laboratories.

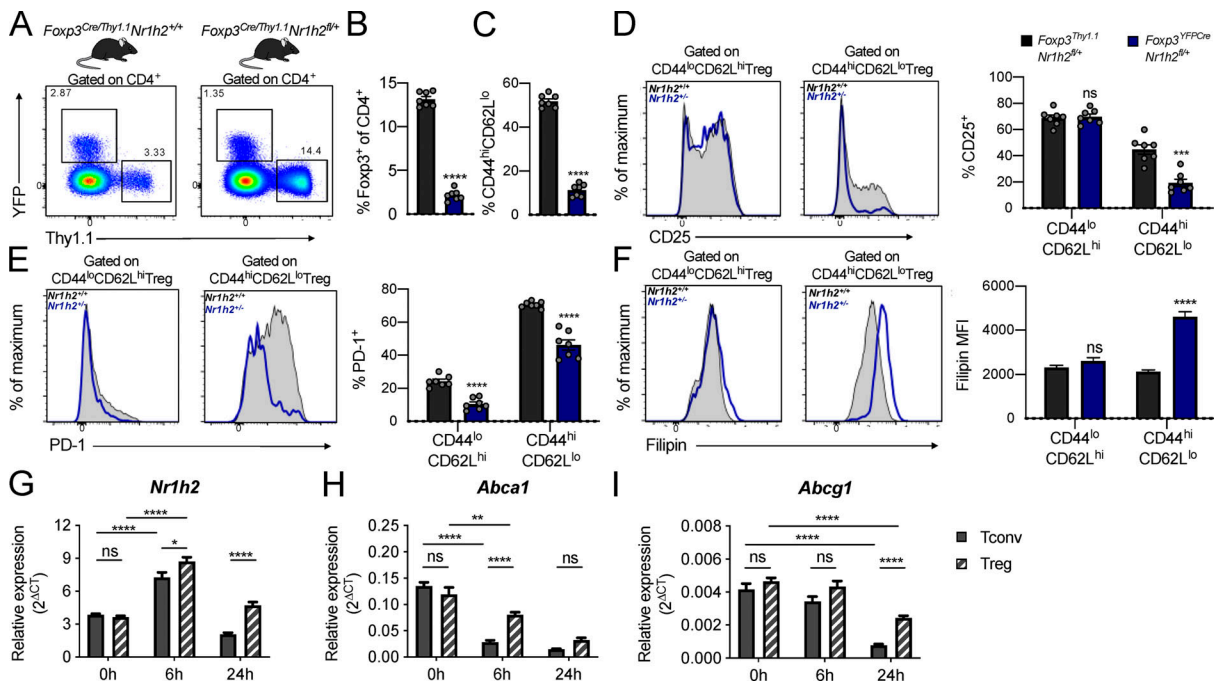


Figure 5. LXRβ-deficient T reg cells are functionally impaired. (A–F) Analysis of 6–8-wk-old *Foxp3^{YFP-Cre/Thy1.1}Nr1h2^{+/-}* mosaic female mice. **(A)** Representative flow cytometry plots showing the percentage of reporter-positive cells in the spleens of *Foxp3^{YFP-Cre/Thy1.1}Nr1h2^{+/-}* (left) and *Foxp3^{YFP-Cre/Thy1.1}Nr1h2^{fl/fl}* mice (right). **(B)** Frequencies of Thy1.1⁺ (*Nr1h2^{+/-}*) and YFP⁺ (*Nr1h2^{-/-}*) splenic T reg cells as a fraction of total CD4⁺ T cells. **(C)** Percentages of activated (CD44^{hi}CD62L^{lo}) cells among Thy1.1⁺ (*Nr1h2^{+/-}*) and YFP⁺ (*Nr1h2^{-/-}*) splenic T reg cells. **(D and E)** Expression of CD25 (D) and PD-1 (E) in the resting (CD44^{lo}CD62L^{hi}) and activated (CD44^{hi}CD62L^{lo}) T reg cell compartments. **(F)** Filipin III staining in the resting and activated T reg cell compartments. **(G–I)** Resting T reg cells (CD4⁺Foxp3⁺) and conventional T cells (CD4⁺Foxp3⁻) isolated from *Foxp3^{GFP}* mice were activated in vitro with CD3 and CD28 antibody-coated beads in the presence of 100 U/ml IL-2. Relative quantification of *Nr1h2* (G), *Abca1* (H), and *Abcg1* (I) mRNA levels by real-time quantitative at 0, 6, and 24 h after activation. Cycle threshold (Ct) values were normalized to β-actin. Data are presented as mean ± SEM (n = 5–7). ns, nonsignificant = P > 0.05; **, P < 0.001; ****, P < 0.0001. Statistical significance was determined using a two-tailed T test (B and C), multiple t tests followed by the Holm-Šidák correction (D–F), or two-way ANOVA followed by the Tukey correction for multiple comparisons (G–I). Data are representative of at least two independent experiments.

Isolation of cells from lymphoid organs, livers, lungs, and colonic lamina propria

For flow cytometric analyses, animals were perfused with a total of 20 ml PBS into both left and right ventricles immediately after euthanasia. Cells were retrieved from spleens, peripheral (brachial, axillary, and inguinal) LNs (pLNs), mesenteric LNs, thymi, and livers by meshing the organs through a 100-μm strainer (Corning; 07-477 201-432) with a syringe plunger. To isolate cells from the colonic lamina propria, colons were first cleaned by flushing the luminal content out with PBS using a syringe, defatted, opened up longitudinally, and diced into 1–2-cm pieces. Tissues were then incubated in 25 ml IEL solution (1× PBS with 2% FBS [ThermoFisher; 35010CV], 10 mM HEPES buffer [ThermoFisher; MT 25-060-CI], 1% penicillin/streptomycin [ThermoFisher; MT 30-002-CI], and 1% L-glutamine [ThermoFisher; MT 25-005-CI] plus 1 mM EDTA [Sigma-Aldrich; E4884] and 1 mM DTT [Sigma-Aldrich; D9779] added immediately before use) for 15 min at 37°C with vigorous shaking (250 rpm) to remove the epithelial fraction. Tissues were then retrieved, washed extensively, and digested in 25 ml LPL solution (1× RPMI 1640 with 2% FBS, 10 mM HEPES buffer, 1% penicillin/streptomycin, 1% L-glutamine, 0.2 U/ml collagenase A [Sigma-Aldrich; 11088793001], and 1 U/ml DNase I [Sigma-Aldrich; 10104159001]) for 30 min at 37°C with vigorous shaking (250 rpm). 0.25-inch ceramic beads (MP Biomedicals; 116540034) were added during

this step (3–4 per sample) to facilitate tissue dissociation. The digested samples were passed through a 100-μm strainer, pelleted at 450 g for 5 min, and washed extensively. Lungs were digested in the same fashion as the lamina propria fraction of the colons for 45 min. Cells from nonlymphoid organs were centrifuged in 40% PBS-adjusted Percoll (vol/vol; ThermoFisher; 45-001-747) in PBS to remove debris. Erythrocytes in the spleen, lung, and liver samples were lysed with ammonium chloride potassium lysis buffer (150 mM NH₄Cl [Sigma-Aldrich; A9434], 10 mM KHCO₃ [Sigma-Aldrich; P7682], and 0.1 mM Na₂EDTA, pH 7.4).

Generation of mixed BM chimeras

Recipient mice (*Tcrb^{-/-}Tcrd^{-/-}*) received a lethal dose (750 cGy) of radiation 24 h before cell transfer. T cell-depleted BM cells from CD4-Cre*Nr1h2^{+/-}*, CD4-Cre*Nr1h2^{fl/+}*, or CD4-Cre*Nr1h2^{fl/fl}* animals (CD45.2⁺) were transferred at a 1:1 ratio to BM cells from congenically marked WT C57BL/6-Ly5.1 donors (CD45.1⁺). 10⁶ BM cells from each genotype (2 × 10⁶ total cells) were transferred into each recipient via the retro-orbital route. Analysis of chimeric mice was performed 8–10 wk after reconstitution.

T cell transfer into lymphopenic hosts

Congenically marked bulk T cells (8 × 10⁶) pooled from the spleen and LNs of adult (8–10 wk old) CD4-Cre*Nr1h2^{+/-}* (CD45.2⁺)

and CD4-Cre*Nrlh2*^{fl/fl} (CD45.1/2⁺) were mixed at a 1:1 ratio and transferred intravenously into *Tcrb*^{-/-}*Tcrd*^{-/-} recipient mice. Animals were sacrificed on day 7 after transfer, and spleens and pLNs were pooled for analysis of T cell activation by flow cytometry.

T cell isolation and purification

Naive (CD44^{lo}CD62L^{hi}CD25^{lo}) CD4⁺ T cells were FACS purified from spleen and pLNs (pooled inguinal, brachial, axial, and submandibular) after a CD4-enrichment step (Invitrogen; Dynabeads 11447D) performed as per manufacturer's instructions. Enriched cell suspensions were stained with antibodies, washed extensively, resuspended in isolation buffer (PBS with 2% FBS, 10 mM Hepes buffer, 1% L-glutamine, and 2 mM EDTA) containing 0.01% SYTOX Blue dead cell stain (ThermoFisher; S34857) to facilitate dead cell exclusion. Naive T cells were sorted on a FACS Aria (BD Biosciences) instrument.

In vitro T cell activation

Sorted T cells (5×10^4) were activated with mouse T activator CD3/CD28 Dynabeads (Gibco) at a 1:1 bead-to-cell ratio in the presence of 100 U/ml IL-2 (Biological Resources Branch, National Cancer Institute) in T cell medium (RPMI 1640 with 10 mM Hepes buffer, 1% penicillin/streptomycin, 1% L-glutamine, 55 μ M β -mercaptoethanol, and 10% FBS) at 37°C/5% CO₂ for the indicated time points. CellTrace Violet (ThermoFisher) labeling was performed according to the manufacturer's instructions. For experiments with HMGCR inhibition, Simva (Sigma-Aldrich; S6196) was added to cell cultures in the presence of mevalonate (Sigma-Aldrich; 79849) or vehicle.

Assessment of cell death

For FasL-induced cell death, naive T cells were activated as described above in the presence of 2.5 μ g/ml recombinant murine FasL (R&D Systems) for 15 min at 37°C/5% CO₂. After washing, cells were resuspended in T cell medium containing 2.5 μ g/ml HA tag antibody (R&D Systems) to promote Fas cross-linking and incubated for 4 h at 37°C/5% CO₂ before analyses. For Fas blocking experiments, naive T cells were activated in the presence of 10 μ g/ml anti-murine FasL antibody (BD Biosciences; clone MFL3) and cultured for 48 h at 37°C/5% CO₂. For dexamethasone-induced cell death, naive T cells were activated in the presence of 1 μ M dexamethasone (Sigma-Aldrich; D-085) or vehicle (methanol) and cultured for 48 h at 37°C/5% CO₂ before analyses.

Flow cytometry

Foxp3 staining was performed using the eBioscience transcription factor staining buffer set (eBioscience). For cytokine production analyses, cells were incubated for 3 h at 37°C/5% CO₂ in restimulation media (complete RPMI 1640 with 5% FBS, 50 ng/ml PMA [Sigma-Aldrich], 500 ng/ml ionomycin [Sigma-Aldrich], 1 μ g/ml brefeldin A [Sigma-Aldrich], and 2 μ M monensin [Sigma-Aldrich]). Extracellular antigens were stained for 15 min at 4°C with an antibody staining mix containing Zombie NIR Fixable Viability dye diluted in PBS. Cells were fixed and permeabilized with BD Cytofix/Cytoperm for 20 min at 4°C.

Antibodies against intracellular antigens were diluted in 1× BD Perm/Wash buffer and cells were stained for 30 min at 4°C. Annexin V APC (BD Biosciences) was diluted 1:100 in Annexin V binding buffer (BD Biosciences) and incubated with cells for 15 min at room temperature after staining of extracellular antigens. Cells were kept in Annexin V buffer before and during FACS analyses. Caspase activity was measured using FITC-conjugated Z-VAD-FMK (Promega) at 1:1,000 dilution. Z-VAD-FMK was incubated with cells at 4°C for 1 h along with antibody staining mix for intracellular antigens. For filipin III staining, cells were fixed with 2% paraformaldehyde for 1 h at room temperature after staining of extracellular antigens. After washing, carryover fixative was quenched with 1.5 mg/ml glycine in PBS for 10 min at room temperature. Cells were washed and then incubated with filipin III solution (Millipore Sigma; 0.05 mg/ml in PBS + 10% FBS) for 2 h at room temperature and washed again before flow cytometric analysis. 123count eBeads (Invitrogen) were added at 10,000 beads/sample to quantify absolute cell numbers. Cytometry data were acquired on an LSRII (Becton Dickinson) or Aurora (Cytex) and analyzed on FlowJo.

Reagents and antibodies

The following clones of fluorescently conjugated or biotinylated antibodies (obtained from BD Biosciences, BioLegend, ThermoFisher, or Tonbo) were used in this study for flow cytometry: anti-CD45 (30-F11), anti-CD3e (17A2), anti-CD90.2 (30-H12), anti-Foxp3 (FJK-16s), anti-TCR β (H57-597), anti-CD90.1 (HIS51), anti-CD4 (RM4-4), anti-CD8 α (53-6.7), anti-GITR (DTA-1), anti-CD44 (IM7), anti-CD62L (MEL-14), anti-CD11b (M1/70), anti-CTLA4 (UC10-4B9), anti-Ki-67 (16A8), anti-CD25 (PC61.5), anti-CD45.1 (A20), anti-CD45.2 (104), anti-IL-2 (JES6-5H4), anti-IL-17A (17B7), anti-IFN γ (XMG1.2), anti-IL-4 (BVD6-24G2), anti-TNF α (MP6-XT22), anti-TCR γ δ (H57-597), anti-Egr2 (erongr2), and anti-PD-1 (J43).

Real-time quantitative PCR

Resting (CD44^{lo}CD62L^{hi}) Foxp3⁺ and Foxp3⁻ CD4⁺ T cells were sorted from *Foxp3*^{GFP} reporter mice and activated in vitro for 6 h as described above. Total RNA was extracted with RNeasy mini kit (Qiagen) according to the manufacturer's instructions. cDNA was synthesized with qScript cDNA Supermix (QuantaBio). Power SYBR Green (ThermoFisher) was used for real-time quantitative PCR reaction in the QuantStudio 6 Flex Real-time PCR system (ThermoFisher). Gene expression was normalized to β -actin transcript levels. Primer sequences were as follows: *Abca1* forward, 5'-AAAACCGCAGACATCCTTCAG-3'; reverse, 5'-CATACCGAACTCGTTCACCC-3'; *Abcg1* forward, 5'-CTTTCCTACTCTGTACCCGAGG-3'; reverse, 5'-CGGGGCATTCCATTGATAAGG-3'; *Nrlh2* forward, 5'-CCAGGAGATTGTGGACTTTGCC-3'; reverse, 5'-TCTGTCTCGTGGTTGTAGCGTC-3'; *Actb* forward, 5'-GTCGAGTCGCGTCCACC-3'; reverse, 5'-GTCATCCATGGCGAACTGGT-3'.

Statistics

P values were calculated with GraphPad Prism 8 using the statistical method denoted in figure legends (one-way ANOVA).

followed by the Holm-Šídák correction, two-way ANOVA followed by Tukey or Holm-Šídák correction, or a two-tailed *t* test). Throughout the study, error bars represent mean ± SEM, and the following notation was used to report statistical significance: ns, nonsignificant = $P > 0.05$; *, $P < 0.05$; **, $P < 0.01$; ***, $P < 0.001$; ****, $P < 0.0001$.

Online supplemental material

Fig. S1 provides in-depth immunophenotyping of T^{ALXR} mice. The spleen, pLNs, mesenteric LNs, colon, liver, lung, and thymus of these mice are profiled. **Fig. S2** contains data showing the activation status of LXRβ-sufficient and -deficient T cells that were cotransferred into lymphopenic hosts. This figure also contains supplementary data derived from mixed BM chimera experiments. **Fig. S3** contains data that demonstrate impaired development of LXRβ-deficient T cells in the thymus of mixed BM chimeric mice.

Acknowledgments

We thank Dr. Frederic Geissmann (Memorial Sloan Kettering Cancer Center, New York, NY) for providing *Nr1h2* floxed mice.

This work was supported by National Institute of Allergy and Infectious Diseases grant RO1 AI034206 (A.Y. Rudensky), the Ludwig Center at Memorial Sloan Kettering Cancer Center, the Parker Institute for Cancer Immunotherapy (A.Y. Rudensky), and a National Cancer Institute predoctoral fellowship (F31 CA254325-01 to A.J. Michaels) and Cancer Center grant P30 CA008748. A.Y. Rudensky is an investigator with the Howard Hughes Medical Institute. R. Bou-Puerto received support from “la Caixa” Foundation (LCF/BQ/AA17/11610016).

Author contributions: A.J. Michaels, C. Campbell, and A.Y. Rudensky conceived the study and wrote the manuscript. A.J. Michaels and C. Campbell performed experiments and analyzed data. R. Bou-Puerto assisted with mixed BM chimera experiments and provided support in drafting and editing of the manuscript.

Disclosures: A.Y. Rudensky reported personal fees from Sonoma Biotherapeutics, RAPT Therapeutics, and Vedanta Biosciences outside the submitted work. No other disclosures were reported.

Submitted: 23 June 2020

Revised: 16 September 2020

Accepted: 16 November 2020

References

Bensinger, S.J., M.N. Bradley, S.B. Joseph, N. Zelcer, E.M. Janssen, M.A. Hausner, R. Shih, J.S. Parks, P.A. Edwards, B.D. Jamieson, and P. Tontonoz. 2008. LXR signaling couples sterol metabolism to proliferation in the acquired immune response. *Cell*. 134:97–111. <https://doi.org/10.1016/j.cell.2008.04.052>

Bettini, M.L., F. Pan, M. Bettini, D. Finkelstein, J.E. Rehg, S. Floess, B.D. Bell, S.F. Ziegler, J. Huehn, D.M. Pardoll, and D.A. Vignali. 2012. Loss of epigenetic modification driven by the Foxp3 transcription factor leads to regulatory T cell insufficiency. *Immunity*. 36:717–730. <https://doi.org/10.1016/j.immuni.2012.03.020>

Bietz, A., H. Zhu, M. Xue, and C. Xu. 2017. Cholesterol Metabolism in T Cells. *Front. Immunol.* 8:1664. <https://doi.org/10.3389/fimmu.2017.01664>

Bookout, A.L., Y. Jeong, M. Downes, R.T. Yu, R.M. Evans, and D.J. Mangelsdorf. 2006. Anatomical profiling of nuclear receptor expression reveals a hierarchical transcriptional network. *Cell*. 126:789–799. <https://doi.org/10.1016/j.cell.2006.06.049>

Buck, M.D., D. O’Sullivan, and E.L. Pearce. 2015. T cell metabolism drives immunity. *J. Exp. Med.* 212:1345–1360. <https://doi.org/10.1084/jem.20151159>

Cui, G., X. Qin, L. Wu, Y. Zhang, X. Sheng, Q. Yu, H. Sheng, B. Xi, J.Z. Zhang, and Y.Q. Zang. 2011. Liver X receptor (LXR) mediates negative regulation of mouse and human Th17 differentiation. *J. Clin. Invest.* 121:658–670. <https://doi.org/10.1172/JCI42974>

Darce, J., D. Rudra, L. Li, J. Nishio, D. Cipolletta, A.Y. Rudensky, D. Mathis, and C. Benoist. 2012. An N-terminal mutation of the Foxp3 transcription factor alleviates arthritis but exacerbates diabetes. *Immunity*. 36:731–741. <https://doi.org/10.1016/j.immuni.2012.04.007>

Fowler, A.J., M.Y. Sheu, M. Schmuth, J. Kao, J.W. Fluhr, L. Rhein, J.L. Collins, T.M. Willson, D.J. Mangelsdorf, P.M. Elias, and K.R. Feingold. 2003. Liver X receptor activators display anti-inflammatory activity in irritant and allergic contact dermatitis models: liver-X-receptor-specific inhibition of inflammation and primary cytokine production. *J. Invest. Dermatol.* 120:246–255. <https://doi.org/10.1046/j.1523-1747.2003.12033.x>

Geltink, R.I.K., R.L. Kyle, and E.L. Pearce. 2018. Unraveling the Complex Interplay Between T Cell Metabolism and Function. *Annu. Rev. Immunol.* 36:461–488. <https://doi.org/10.1146/annurev-immunol-042617-053019>

Gimpl, G. 2010. Cholesterol-protein interaction: methods and cholesterol reporter molecules. *Subcell. Biochem.* 51:1–45. https://doi.org/10.1007/978-90-481-8622-8_1

Hindinger, C., D.R. Hinton, S.J. Kirwin, R.D. Atkinson, M.E. Burnett, C.C. Bergmann, and S.A. Stohman. 2006. Liver X receptor activation decreases the severity of experimental autoimmune encephalomyelitis. *J. Neurosci. Res.* 84:1225–1234. <https://doi.org/10.1002/jnr.21038>

Howie, D., A. Ten Bokum, A.S. Necula, S.P. Cobbold, and H. Waldmann. 2018. The Role of Lipid Metabolism in T Lymphocyte Differentiation and Survival. *Front. Immunol.* 8:1949. <https://doi.org/10.3389/fimmu.2017.01949>

Jakobsson, T., L.L. Vedin, T. Hassan, N. Venteclef, D. Greco, M. D’Amato, E. Treuter, J.A. Gustafsson, and K.R. Steffensen. 2014. The oxysterol receptor LXRβ protects against DSS- and TNBS-induced colitis in mice. *Mucosal Immunol.* 7:1416–1428. <https://doi.org/10.1038/mi.2014.31>

Josefowicz, S.Z., L.F. Lu, and A.Y. Rudensky. 2012. Regulatory T cells: mechanisms of differentiation and function. *Annu. Rev. Immunol.* 30:531–564. <https://doi.org/10.1146/annurev-immunol.25.022106.141623>

Klammt, C., and B.F. Lillemeier. 2012. How membrane structures control T cell signaling. *Front. Immunol.* 3:291. <https://doi.org/10.3389/fimmu.2012.00291>

Lee, P.P., D.R. Fitzpatrick, C. Beard, H.K. Jessup, S. Lehar, K.W. Makar, M. Pérez-Melgosa, M.T. Sweetser, M.S. Schlissel, S. Nguyen, et al. 2001. A critical role for Dnmt1 and DNA methylation in T cell development, function, and survival. *Immunity*. 15:763–774. [https://doi.org/10.1016/S1074-7613\(01\)00227-8](https://doi.org/10.1016/S1074-7613(01)00227-8)

Legembre, P., S. Daburon, P. Moreau, J.F. Moreau, and J.L. Taupin. 2006. Modulation of Fas-mediated apoptosis by lipid rafts in T lymphocytes. *J. Immunol.* 176:716–720. <https://doi.org/10.4049/jimmunol.176.2.716>

Levine, A.G., A. Arvey, W. Jin, and A.Y. Rudensky. 2014. Continuous requirement for the TCR in regulatory T cell function. *Nat. Immunol.* 15:1070–1078. <https://doi.org/10.1038/ni.3004>

Liston, A., K.M. Nutsch, A.G. Farr, J.M. Lund, J.P. Rasmussen, P.A. Koni, and A.Y. Rudensky. 2008. Differentiation of regulatory Foxp3+ T cells in the thymic cortex. *Proc. Natl. Acad. Sci. USA.* 105:11903–11908. <https://doi.org/10.1073/pnas.0801506105>

Muller, C.P., D.A. Stephany, D.F. Winkler, J.M. Hoeg, S.J. Demosky Jr., and J.R. Wunderlich. 1984. Filipin as a flow microfluorometry probe for cellular cholesterol. *Cytometry*. 5:42–54. <https://doi.org/10.1002/cyto.990050108>

Pearce, E.L. 2010. Metabolism in T cell activation and differentiation. *Curr. Opin. Immunol.* 22:314–320. <https://doi.org/10.1016/j.coi.2010.01.018>

Rubtsov, Y.P., J.P. Rasmussen, E.Y. Chi, J. Fontenot, L. Castelli, X. Ye, P. Treuting, L. Siewe, A. Roers, W.R. Henderson Jr., et al. 2008. Regulatory T cell-derived interleukin-10 limits inflammation at environmental interfaces. *Immunity*. 28:546–558. <https://doi.org/10.1016/j.immuni.2008.02.017>

Schulman, I.G. 2017. Liver X receptors link lipid metabolism and inflammation. *FEBS Lett.* 591:2978–2991. <https://doi.org/10.1002/1873-3468.12702>

Shi, J., and H.T. Petrie. 2012. Activation kinetics and off-target effects of thymus-initiated cre transgenes. *PLoS One.* 7:e46590. <https://doi.org/10.1371/journal.pone.0046590>

- Vahl, J.C., C. Drees, K. Heger, S. Heink, J.C. Fischer, J. Nedjic, N. Ohkura, H. Morikawa, H. Poeck, S. Schallenberg, et al. 2014. Continuous T cell receptor signals maintain a functional regulatory T cell pool. *Immunity*. 41:722–736. <https://doi.org/10.1016/j.immuni.2014.10.012>
- van der Veecken, J., A.J. Gonzalez, H. Cho, A. Arvey, S. Hemmers, C.S. Leslie, and A.Y. Rudensky. 2016. Memory of Inflammation in Regulatory T Cells. *Cell*. 166:977–990. <https://doi.org/10.1016/j.cell.2016.07.006>
- Wang, B., and P. Tontonoz. 2018. Liver X receptors in lipid signalling and membrane homeostasis. *Nat. Rev. Endocrinol.* 14:452–463. <https://doi.org/10.1038/s41574-018-0037-x>
- Xiong, N., and D.H. Raulet. 2007. Development and selection of gammadelta T cells. *Immunol. Rev.* 215:15–31. <https://doi.org/10.1111/j.1600-065X.2006.00478.x>
- Xu, J., G. Wagoner, J.C. Douglas, and P.D. Drew. 2009. Liver X receptor agonist regulation of Th17 lymphocyte function in autoimmunity. *J. Leukoc. Biol.* 86:401–409. <https://doi.org/10.1189/jlb.1008600>

Supplemental material

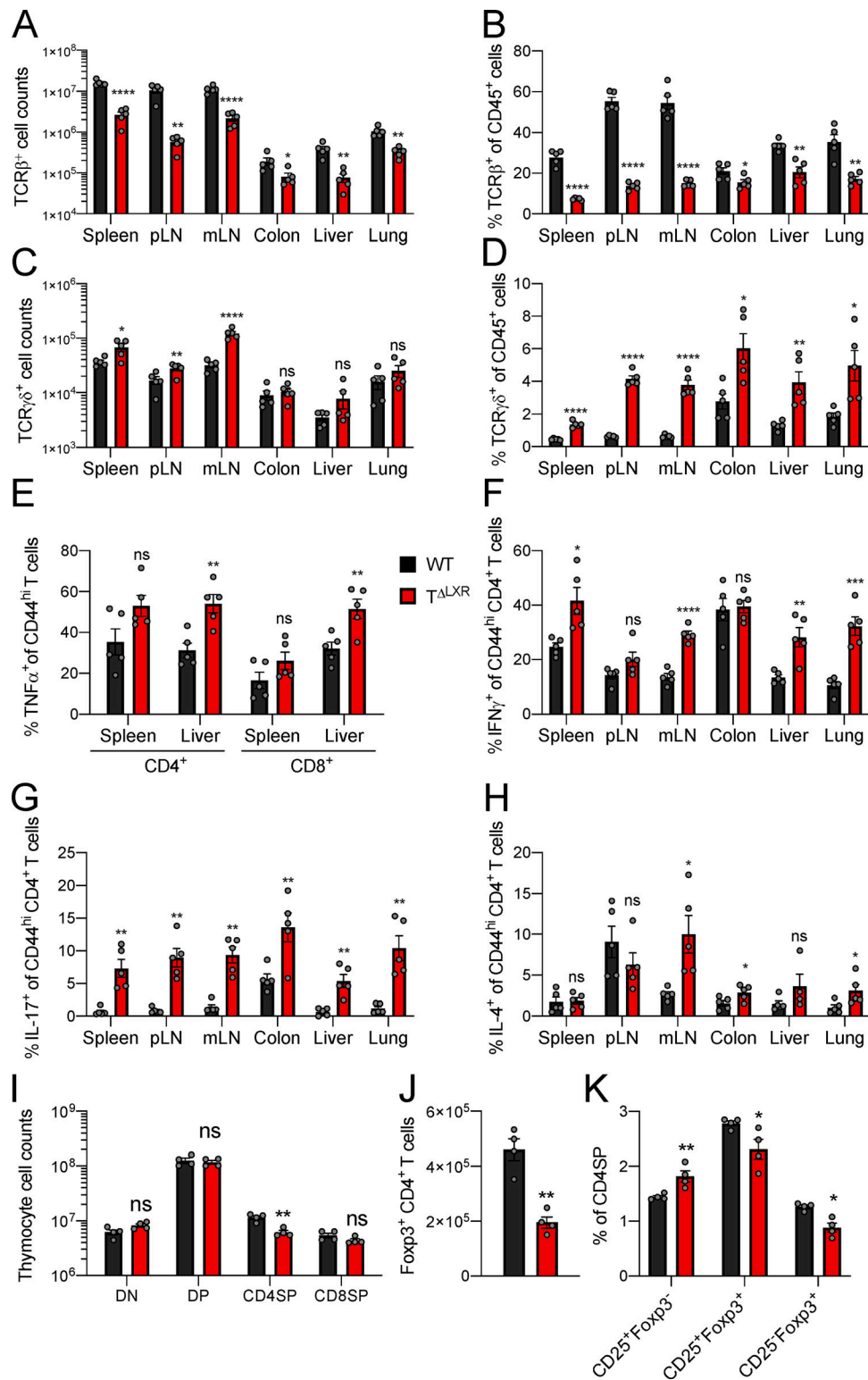


Figure S1. **Analysis of 6–8-wk-old CD4-CreNr1h2^{R/R} (T^{ΔLXR}) and Nr1h2^{R/R} (WT) littermate mice.** (A) Quantification of TCRβ⁺ T cell numbers in indicated tissues. (B) Percentages of TCRβ⁺ T cells as a fraction of total CD45⁺ immune cells across indicated tissues. (C) Quantification of TCRγδ⁺ T cell numbers. (D) Percentages TCRγδ⁺ T cells among CD45⁺ cells. (E–H) Frequencies of effector T cells producing the indicated cytokines upon ex vivo restimulation with PMA and ionomycin in the presence of brefeldin A and monensin. (E) Percentages of CD4⁺ and CD8⁺ effector T cells producing TNFα. (F–H) Percentages of effector CD4⁺ T cells producing IFNγ (F), IL-17 (G), or IL-4 (H) in indicated organs. (I) Quantification of cell numbers within the indicated thymocyte subset. (J) Quantification of thymic CD4⁺Foxp3⁺ cells. (K) Frequencies of thymic T reg cell precursor subsets among CD4SP cells. Data are presented as mean ± SEM (n = 5). ns, nonsignificant = P > 0.05; *, P < 0.05; **, P < 0.01; ***, P < 0.001; ****, P < 0.0001. Statistical significance was determined using a two-tailed T test (J) or multiple t tests followed by the Holm-Šidák correction (A–I and K). Data are representative of at least three independent experiments. mLN, mesenteric LN.

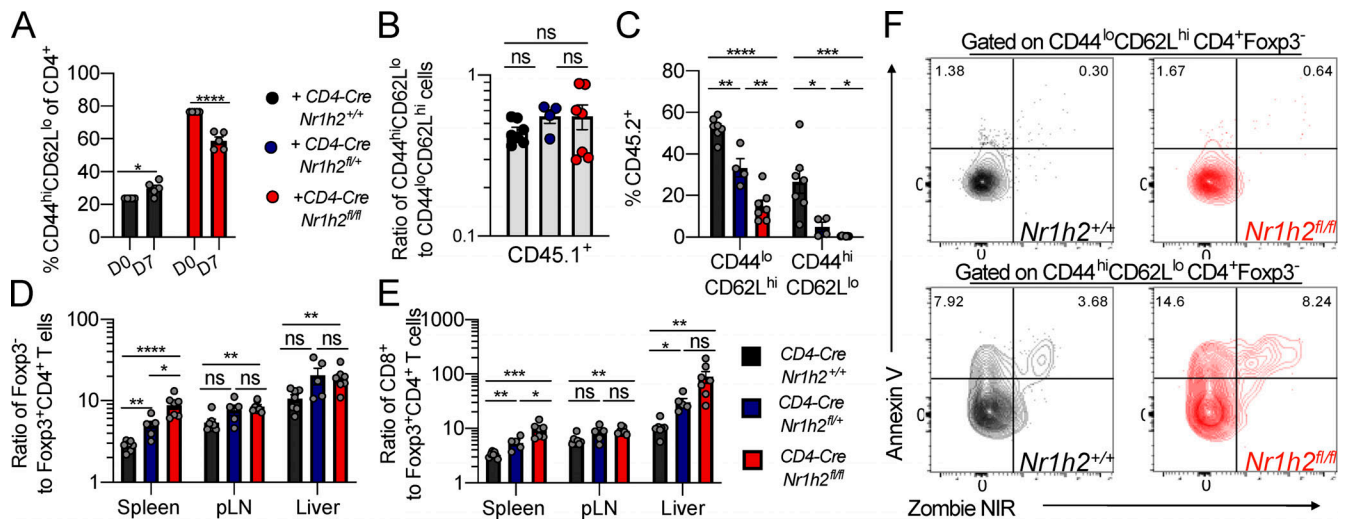


Figure S2. **Analysis of cell-intrinsic effects of Nr1h4 deficiency on peripheral T cells in mixed BM chimeras.** (A) Bulk T cells from CD4-CreNr1h2^{+/+} (CD45.2⁺) and CD4-CreNr1h2^{fl/fl} (CD45.1/2⁺) were mixed at a 1:1 ratio and transferred into *Tcrb*^{-/-}*Tcrd*^{-/-} recipient mice. Percentages of activated (CD44^{hi}CD62L^{lo}) CD4⁺ T cells at day 7 after transfer. (B–F) CD45.2⁺ BM (BM) precursor cells from CD4-CreNr1h2^{+/+}, CD4-CreNr1h2^{fl/fl}, or CD4-CreNr1h2^{fl/fl} animals were mixed at a 1:1 ratio with CD45.1⁺ calibrator cells from WT donors and transferred into lethally irradiated mice. Spleens of recipients were analyzed 8 wk after reconstitution. (B) Percentage of activated (CD44^{hi}CD62L^{lo}) cells among WT CD4⁺ T cells from the calibrator donor (CD45.1⁺). (C) Contribution of CD45.2⁺ cells with the indicated genotype to the effector (CD44^{hi}CD62L^{lo}) or naive (CD44^{lo}CD62L^{hi}) CD4⁺ T cell pool. (D) Ratios of Foxp3⁻ to Foxp3⁺ CD4⁺ T cell numbers within the CD45.2⁺ compartment. (E) Ratios of CD8⁺ to CD4⁺Foxp3⁺ T cell numbers within the CD45.2⁺ compartment. (F) Representative flow cytometry plots of Annexin V staining of effector and naive CD4⁺ T cells from the spleen of mixed chimeric mice. Data are presented as mean ± SEM (*n* = 4–7). ns, nonsignificant = *P* > 0.05; *, *P* < 0.05; **, *P* < 0.01; ***, *P* < 0.001; ****, *P* < 0.0001. Statistical significance was determined using multiple *t* tests (A) or one-way ANOVA (B–F) followed by the Holm-Šidák correction. Data are representative of at least two independent experiments.

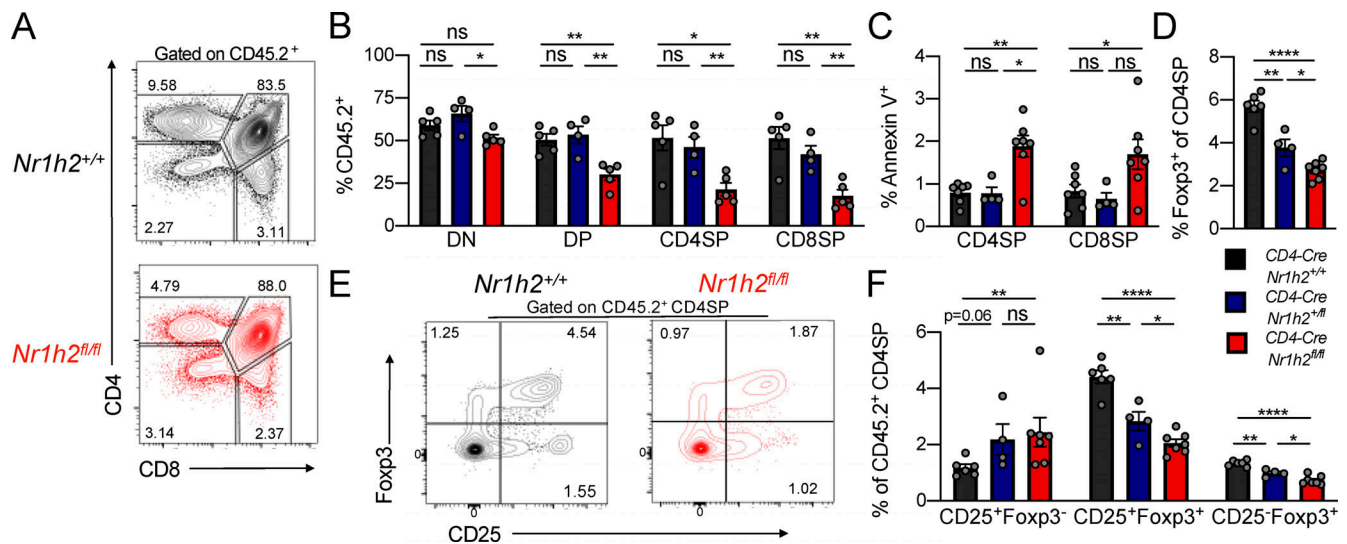


Figure S3. **Analysis of cell-intrinsic effects of Nr1h4 deficiency on T cell differentiation in the thymus.** CD45.2⁺ BM precursor cells from CD4-CreNr1h2^{+/+}, CD4-CreNr1h2^{fl/fl}, or CD4-CreNr1h2^{fl/fl} animals were mixed at a 1:1 ratio with CD45.1⁺ calibrator cells from WT donors and transferred into lethally irradiated mice. Thymi of recipient mice were analyzed 8 wk after reconstitution. (A) Representative flow cytometry plots comparing CD4-CreNr1h2^{+/+} and CD4-CreNr1h2^{fl/fl} T cell development. (B) Contribution of CD45.2⁺ cells with the indicated genotype to the DN, DP, CD4SP, and CD8SP populations. (C) Frequencies of Annexin V⁺ cells among CD45.2⁺ CD4SP and CD8SP thymocyte subsets. (D) Frequencies of Foxp3⁺ cells among CD45.2⁺ CD4SP thymocytes. (E and F) Representative flow cytometry plot (E) and quantification (F) of T reg cell precursor subsets among CD45.2⁺ CD4SP cells. Data are presented as mean ± SEM (*n* = 4–7). ns, nonsignificant = *P* > 0.05; *, *P* < 0.05; **, *P* < 0.01; ****, *P* < 0.0001. Statistical significance was determined using one-way ANOVA followed by the Holm-Šidák correction. Data are representative of three independent experiments.